Available online at www.sciencedirect.com
SCIENCE DIRECT®
Journal of Non-Crystalline Solids 345&346 (2004) 343–348
JOURNAL OF NON-CRYSTALLINE SOLIDS
www.elsevier.com/locate/jnoncrysol

Rare-earth doped tungsten tellurite glasses and waveguides: fabrication and characterization

G. Nunzi Conti [a,b,*,1], S. Berneschi [b], M. Bettinelli [c], M. Brenci [b], B. Chen [d], S. Pelli [b], A. Speghini [c], G.C. Righini [b]

[a] Centro di Eccellenza Optronica, Largo Fermi 6, I-50125 Firenze, Italy
[b] Department of Optoelectronics and Photonics, Nello Carrara Institute of Applied Physics, IFAC - CNR, Via Panciatichi 64, I-50127 Firenze, Italy
[c] Scientific and Technological Department, Università di Verona, Strada le Grazie 15, 37134 Verona, Italy
[d] Changchun Institute of Optics, Fine Mechanics and Physics, CIOMP-CAS, Changchun 130022, Jilin, People's Republic of China

Available online 23 September 2004

Abstract

Tungsten tellurite glasses doped with Er^{3+}, Tm^{3+}, Pr^{3+}, and Ho^{3+} ions were prepared by melt quenching. The glass matrix was the same for all types of glasses and had a high sodium content in order to allow the fabrication of waveguides using an ion-exchange technique. The absorption spectra of the glasses were measured and the Judd–Ofelt parameters Ω_q were obtained from the experimental oscillator strengths of the $f \rightarrow f$ transitions. Er^{3+} doped glasses showed a very high quantum efficiency when comparing the calculated radiative decay time with the measured lifetime of the $^4I_{13/2}$ metastable level. $Ag^+ \leftrightarrow Na^+$ ion-exchanged planar waveguides were successfully obtained in all types of glasses and characterized by the prism coupling technique. It turned out that the diffusion constant values are very similar for glasses containing different rare-earth ions with the same concentration, while, at least for the Er^{3+} doped ones, the diffusion constant changes with the ions concentration.

PACS: 42.70.Ce; 42.82.Et; 78.66.Jg; 82.65.F

1. Introduction

Tellurite glasses have recently gained a wide attention because of their potential as hosts of rare-earth elements for the development of fiber and integrated optic amplifiers and lasers covering all the main telecommunication bands. In fact, while Nd^{3+} or Pr^{3+} doped glasses can cover the 1.3 μm band (O band) [1,2], Tm^{3+}, Tm^{3+}-Ho^{3+}, and Er^{3+} doped glasses have been used for amplification in the S, C and L band between 1.46 and 1.61 μm [3–5]. Tellurite glasses have the lowest phonon energy (about 780 cm^{-1}) among oxide glass formers leading to fluorescence from additional energy levels compare to silicate or phosphate glasses and they also offer good stability and chemical durability. Furthermore, they exhibit high refractive index, a wide transmission range (0.35–5 μm), low process temperature and significant non-linear properties [6–8].

Glass integrated optics can offer excellent flexibility to accommodate more functions and it is suitable to cost effective mass production. Integrated optical lasers and amplifiers have been obtained using rare earth-doped glasses exploiting different technologies [9]. Among them ion-exchange has been recognized as a valuable technique for the fabrication of active devices allowing high optical gain per unit length [10,11].

There are only a few papers reporting the fabrication of waveguides in tellurite glasses [12,13] even though

* Corresponding author. Tel.: +39 055 423 5243; fax: +39 055 423 5352.
E-mail address: g.nunziconti@ifac.cnr.it (G. Nunzi Conti).
[1] Present address: Via Panciatichi 64, I-50127 Firenze, Italy.

0022-3093/$ - see front matter © 2004 Elsevier B.V. All rights reserved.
doi:10.1016/j.jnoncrysol.2004.08.041

Table 1
Molar composition and measured refractive index $n(\pm 0.001)$ of the nine glasses investigated in this work

Sample	WO_3	Na_2O	TeO_2	Er_2O_3	Ho_2O_3	Pr_6O_{11}	Tm_2O_3	n @ 635 nm
WNT	25	15	60					2.046
WNT*Er*005	25	15	60	0.05				2.047
WNT*Er*05	25	15	60	0.5				2.045
WNT*Er*10	25	15	60	1.0				2.039
WNT*Er*15	25	15	60	1.5				2.036
WNT*Er*20	25	15	60	2.0				2.032
WNT*Ho*	25	15	60		1			2.037
WNT*Pr*	25	15	60			0.33		2.041
WNT*Tm*	25	15	60				1	2.038

some theoretical analysis predicts that waveguide amplifiers in tellurite glass can exhibit improved gain characteristics [14]. Here we describe our results in the characterization of planar ion-exchanged optical waveguides in various glasses, all based on a tungsten–tellurite matrix doped with different rare earth ions (Er^{3+}, Tm^{3+}, Pr^{3+}, and Ho^{3+}); we also report on some of the spectroscopic properties of these glasses.

2. Experimental

A total of nine different tungsten-tellurite glasses with high sodium content and doped with four different types of rare earth ions (Er^{3+}, Tm^{3+}, Pr^{3+}, and Ho^{3+}) were fabricated. Table 1 lists the molar composition and the value of the refractive index (at 635 nm) of the various samples including the undoped glass matrix and five glasses having different Er_2O_3 contents. WNT*Er*10, WNT*Ho*, WNT*Pr*, and WNT*Tm* glasses have the same rare-earth ions concentration ($\sim 4 \times 10^{20}$ ions/cm^3). They were all prepared by melting batches composed of analytical grade of the constituents (WO_3, Na_2CO_3, TeO_2, and Er_2O_3 or Ho_2O_3 or Pr_6O_{11} or Tm_2O_3) in a platinum crucible for 2 h at 750 °C. The glasses were then quenched in air on a stainless steel plate and annealed for 2 h at 360 °C. Finally the samples, with a typical size of $2 \times 2 \times 0.3$ cm^3, were carefully polished for the optical measurements and waveguide fabrication.

Absorption spectra in the visible and near infrared regions were measured at room temperature by a double beam spectrometer with a resolution of 1 nm. Emission spectra of the WNT*Er* samples around 1.5 μm were detected using as excitation source a semiconductor laser at 976 nm: luminescence was dispersed using a monochromator with a resolution of 1 nm and detected using InGaAs photodiode and lock-in technique. The lifetime of the $^4I_{13/2}$ level was also measured after excitation at 976 nm. For these measurements the samples were made thinner than 1 mm to minimize reabsorption.

As a source to perform the ion-exchange process we used an eutectic solution of $AgNO_3$, KNO_3, and $NaNO_3$ with weight percentage of 2, 43, and 55, respectively; this solution has a melting temperature of about 240 °C. Reagent grade nitrates were weighted, mixed and placed in stainless steel crucibles. The ion-exchange temperature used in this work was 330 °C.

Surface quality of the processed samples was visually inspected with a microscope and the roughness was measured using a surface profiler. The effective indices of the waveguide modes were measured at 635 nm using prism coupling technique with an in-house developed semi-automatic system (COMPASSO); the same instrument was used to measure the refractive indices of the bulk glass samples (reported in Table 1). Finally, the index profile of the waveguides in the ion-exchanged samples was calculated from the measured mode indices using the inverse WKB method [15].

3. Results

3.1. Glass characterization: Judd–Ofelt analysis

In the framework of the Judd–Ofelt theory [16] the theoretical oscillator strengths P for the forced electric dipole transitions are expressed as a sum of transition matrix elements, involving three Judd–Ofelt intensity parameters Ω_q ($q = 2, 4, 6$), which depends on the host matrix. These parameters were determined by using a least-squares fitting approach to the measured absorption bands corresponding to $4f^N \rightarrow 4f^N$ transitions from the ground state to the higher level. Table 2 lists the obtained values of Ω_q for the four glasses together with the root mean square deviations δ_{rms} of the oscillator strengths, calculated as following:

$$\delta_{rms} = \left[\sum (\Delta P)^2/(n_t - 3)\right]^{1/2}.$$

Table 2
Intensity parameters Ω_q and root mean square deviations δ of the oscillator strengths calculated for the four different tellurite glasses

Glass	Ω_2 (pm^2)	Ω_4 (pm^2)	Ω_6 (pm^2)	δ_{rms} (10^{-8})
WNT*Er*10	6.7	1.7	1.15	19
WNT*Ho*	5.7	4.0	1.0	80
WNT*Pr*	6.9	3.5	5.2	196
WNT*Tm*	5.8	0.85	1.45	43

Table 3
Calculated spontaneous emission probability A_{ij}, branching ratios β_{ij} and radiative lifetime τ_R for the main emitting states of the four rare earth ions in the tellurite glasses

Initial levels	Final levels	A_{ij} (S^{-1})		β_{ij} (%)	τ_R (ms)
		E-D	M-D		
WNTEr glass					
$^4F_{5/2}$	$^4F_{7/2}$	3.38	2.25	0.08	0.15
	$^2H_{11/2}$	9.04		0.13	
	$^4S_{3/2}$	3.27		0.04	
	$^4F_{9/2}$	277.3		4.22	
	$^4I_{9/2}$	306.4		4.67	
	$^4I_{11/2}$	312.9		4.77	
	$^4I_{13/2}$	2789		42.52	
	$^4I_{15/2}$	2855		43.53	
$^4F_{7/2}$	$^2H_{11/2}$	2.69		0.03	0.12
	$^4S_{3/2}$	0.07		~0.00	
	$^4F_{9/2}$	17.71	41.64	0.68	
	$^4I_{9/2}$	317.4		3.65	
	$^4I_{11/2}$	568.9		6.55	
	$^4I_{13/2}$	1253		14.42	
	$^4I_{15/2}$	6483		74.65	
$^2H_{11/2}$	$^4S_{3/2}$	0.07		~0.00	0.05
	$^4F_{9/2}$	78.35		0.36	
	$^4I_{9/2}$	277.0		1.30	
	$^4I_{11/2}$	195.2		0.91	
	$^4I_{13/2}$	336.1		1.58	
	$^4I_{15/2}$	20372		95.82	
$^4S_{3/2}$	$^4F_{9/2}$	1.24		0.03	0.27
	$^4I_{9/2}$	141.8		3.84	
	$^4I_{11/2}$	83.5		2.26	
	$^4I_{13/2}$	1014		27.52	
	$^4I_{15/2}$	2443		66.32	
$^4F_{9/2}$	$^4I_{9/2}$	12.37		0.35	0.28
	$^4I_{11/2}$	70.67		2.00	
	$^4I_{13/2}$	179.8		5.10	
	$^4I_{15/2}$	3257		92.53	
$^4I_{9/2}$	$^4I_{11/2}$	2.17	4.98	1.60	2.24
	$^4I_{13/2}$	104.7		23.51	
	$^4I_{15/2}$	333.6		74.88	
$^4I_{11/2}$	$^4I_{13/2}$	43.82	23.24	12.10	2.57
	$^4I_{15/2}$	341.9		87.90	
$^4I_{13/2}$	$^4I_{15/2}$	209.3	85.95	100	3.39
WNTHo glass					
$^3F_5$	$^5I_4$	0.16		0.00	0.18
	$^5I_5$	13.19		0.23	
	$^5I_6$	179.5		3.21	
	$^5I_7$	1086		19.43	
	$^5I_8$	4309		77.11	
$^5I_4$	$^5I_5$	8.91	5.25	10.78	7.38
	$^5I_6$	50.40		37.2	
	$^5I_7$	59.20		43.7	
	$^5I_8$	11.25		8.3	
$^5I_5$	$^5I_6$	13.20	12.25	10.61	4.17
	$^5I_7$	117.6		49.05	
	$^5I_8$	96.73		40.33	
$^5I_6$	$^5I_7$	31.38	26.75	18.85	3.24
	$^5I_8$	250.3		81.15	
$^5I_7$	$^5I_8$	109.2	46.66	100.0	6.42

(*continued on next page*)

Table 3 (*continued*)

Initial levels	Final levels	A_{ij} (S^{-1})		β_{ij} (%)	τ_R (ms)
		E-D	M-D		
WNTTm glass					
$^1G_4$	$^3F_2$	22.71		0.45	0.20
	$^3F_3$	109.2		2.21	
	$^3H_4$	583.2		11.80	
	$^3H_5$	1676		33.92	
	$^3F_4$	342.5		6.93	
	$^3H_6$	2206		44.66	
$^3F_2$	$^3F_3$	0.02	0.07	0.00	0.28
	$^3H_4$	33.01		0.92	
	$^3H_5$	398.1		11.13	
	$^3F_4$	1723		48.19	
	$^3H_6$	1420		39.73	
$^3F_3$	$^3H_4$	6.09	1.29	0.16	0.22
	$^3H_5$	766.9		17.06	
	$^3F_4$	141.1		3.13	
	$^3H_6$	3580		79.63	
$^3H_4$	$^3H_5$	26.44		0.83	0.31
	$^3F_4$	234.8		7.38	
	$^3H_6$	2917		91.77	
$^3H_5$	$^3F_4$	15.52	3.17	3.04	1.62
	$^3H_6$	484.7	112.7	96.96	
$^3F_4$	$^3H_6$	459.4		100	2.18
WNTPr glass					
$^3P_0$	$^1D_2$	38.23		0.03	0.01
	$^1G_4$	1188		1.17	
	$^3F_4$	7028		6.96	
	$^3F_3$	0.00		0.00	
	$^3F_2$	49486		49.03	
	$^3H_6$	10350		10.25	
	$^3H_5$	0.00		0.00	
	$^3H_4$	32822		32.52	
$^1D_2$	$^1G_4$	1422		14.60	0.10
	$^3F_4$	4575		46.97	
	$^3F_3$	377.2		3.87	
	$^3F_2$	769.6		7.90	
	$^3H_6$	624.2		6.40	
	$^3H_5$	32.33		0.33	
	$^3H_4$	1938		19.90	
$^1G_4$	$^3F_4$	44.05		3.83	0.87
	$^3F_3$	7.20		0.62	
	$^3F_2$	5.05		0.43	
	$^3H_6$	342.4		29.80	
	$^3H_5$	691.3		60.18	
	$^3H_4$	58.71		5.11	
$^3F_4$	$^3F_3$	0.02	0.01	0.00	0.98
	$^3F_2$	1.99		0.19	
	$^3H_6$	103.0		10.08	
	$^3H_5$	298.2		29.19	
	$^3H_4$	618.2		60.52	
$^3F_3$	$^3F_2$	0.78	0.60	0.04	0.60
	$^3H_6$	44.94		2.69	
	$^3H_5$	389.1		23.36	
	$^3H_4$	1229		73.85	

ΔP is the difference between the experimental and theoretical oscillator strengths for an absorption transition, n_t is the number of transitions involved into the Judd–Ofelt calculation and $\sum$ runs over the transitions considered in the Judd–Ofelt calculation. These values were used to calculate the spontaneous emission probabilities A_{ij}, the branching ratios β_{ij}, and the radiative lifetime τ_R between the most important energy levels of the four rare earth ions in our tellurite glasses: the complete data are reported in Table 3.

For the Er^{3+} doped glasses (WNT*Er* glasses) the experimental lifetime values (τ_{exp}) of the $^4I_{13/2}$ level were ranging from 3.4 ± 0.2 ms in the WNT*Er*005 glass (lowest concentration: 2×10^{19} ions/cm^3) to 1.5 ± 0.2 ms in the WNT*Er*20 glass (highest concentration: 8×10^{20} ions/cm^3): a reduction in lifetime occurs for increasing Er^{3+} concentration because of concentration quenching. Correspondingly the quantum efficiency η ($\eta = \tau_{exp}/\tau_R$) varied from 100% to 45%: it is noteworthy to point out that in the WNT*Er* 05 glass which has relatively high ions concentration (2×10^{20} ions/cm^3) the quantum efficiency is still more than 80% (τ_{exp} = 2.8 ± 0.2 ms). A large effective emission cross section bandwidth of 62 nm was also measured.

3.2. Ion exchanged waveguide characterization

By using a surface profiler we observed no major changes in the surface roughness of the glasses due to the ion-exchange process. Subsequently, the presence of guided modes was checked by using a rutile prism to couple light into the waveguides. We indeed obtained planar waveguides in all the samples. We fabricated multimode waveguides with up to 8 modes at 635 nm in order to use the inverse WKB (IWKB) method to determine the refractive index profile resulting from the ion-exchange process. We found out that the analytical function describing the index profile n that better fits the measured effective indices is:

$$n(x) = n_{sub} + (n_{max} - n_{sub}) \exp(-x^3/d^3) = n_{sub} + \Delta n_{max} \exp(-x^3/d^3),$$

where x is the depth coordinate, n_{sub} is the index of the glass substrate, n_{max} is the index at the surface and d is the effective depth of the waveguide. d is related to the diffusion time t (length of the process) by the equation $d = (Dt)^{1/2}$, where D is an effective diffusion coefficient that depends on the molten salt solution, the glass and the temperature. Table 4 lists the number of modes, diffusion coefficient D and maximum index change Δn_{max} at 635 nm for each of the nine samples we exchanged under the same process conditions: 330 °C for 90 min in the same eutectic solution. We observed a very high surface index change ($\Delta n_{max} \sim 0.13$), which is almost the same (within less than 10%) for all types of glasses. Diffusion coefficients are also very similar (within less than 10% as well) for glasses containing the same rare-earth ions concentration (WNT*Er*10, WNT*Ho*, WNT*Pr* and WNT*Tm* glasses). As a consequence index profiles of waveguides obtained in these latter glasses under the same process conditions are very similar, as shown in Fig. 1. On the contrary, as we also reported elsewhere [17] and as shown in Fig. 1, diffusion coefficients are strongly affected by Er^{3+} ions concentration.

Table 4
Diffusion constants and maximum index changes of the nine glasses after a 90 min ion-exchange at 330 °C in a $AgNO_3$:KNO_3:$NaNO_3$ (2:43:55 w.%) solution

Sample	Modes @ 635 nm	D_e (10^{-4} μm^2/s) ± 5%	Δn_{max} (±0.002) @ 635 nm
WNT	8	16.6	0.125
WNT*Er*005	7	14.6	0.125
WNT*Er*05	6	9.9	0.1235
WNT*Er*10	6	9.8	0.128
WNT*Er*15	5	7.3	0.134
WNT*Er*20	5	6.0	0.1275
WNT*Ho*	6	10.4	0.132
WNT*Pr*	6	10.6	0.125
WNT*Tm*	6	9.8	0.131

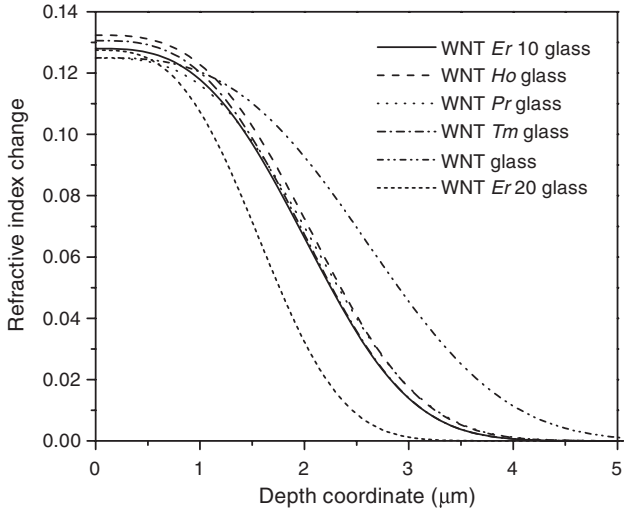

Fig. 1. Calculated index profiles at 635 nm of the waveguides obtained in six different glasses after a 90 min ion-exchange at 330 °C in a $AgNO_3$:KNO_3:$NaNO_3$ (2:43:55 wt%) solution.

4. Discussion

The goal of this work was to study rare-earth doped tellurite glasses that could be used to fabricate ion-exchanged integrated waveguides. We chose a tungsten tellurite matrix doped with sodium: in fact by adding WO_3 to TO_2 the transition temperature T_g of the glass

increases (T_g for WNT glass is 356 °C while, as example, for zinc tellurite glasses it is below 300 °C [17]), allowing a wider range of temperature and shorter times to perform ion-exchange. The chemical durability was also very good while on the contrary glass stability is relatively poor as onset crystallization temperature T_c is around 390 °C, which is very close to T_g [12].

Judd–Ofelt parameters for the Er^{3+} doped glasses (WNT*Er* glasses) were not dependent on the ion concentration and were very similar to those reported in the literature [6] for zinc tellurite glasses. The values of Ω_6 for the Tm^{3+} and Pr^{3+} doped glasses (WNT*Tm* and WNT*Pr*) are also similar to those published in Ref. [3,4,6] for zinc tellurite and sodium zinc tellurite glasses; the values of Ω_4 are instead lower while those of Ω_2, which indicates the degree of covalency, are higher in our glasses.

A final comment regards the decrease of the ion exchange diffusion coefficients with increasing Er^{3+} ions concentration. A possible reason for this 'slowing down' of the diffusion process is probably related to the increased stability and rigidity of tellurite glass when doped with Er^{3+} or another rare earth as indicated in reference [18]: more stable glass would be more reluctant to loose Na^+ from its structure.

5. Conclusions

Tungsten sodium tellurite glasses doped with Tm^{3+}, Pr^{3+}, Ho^{3+}, and various concentrations of Er^{3+} were fabricated and the optical transitions of the rare earth ions were investigated. The measured absorption spectra were analysed by Judd–Ofelt theory and the intensity parameters were estimated. Comparison between calculated and measured lifetime showed a quantum efficiency higher than 80% for the Er^{3+} doped samples with concentration up to 2×10^{20} ions/cm^3.

Planar waveguides were successfully fabricated in all types of glasses by a $Ag^+ \leftrightarrow Na^+$ ion-exchange technique. Characterization of the diffusion process showed that the maximum index change at the glass surface of these glasses does not depend on the type and concentration of rare earth while the diffusion depth of the Ag^+ ions is affected by the ion concentration but not by the ion type.

Acknowledgments

This work was partially supported by MIUR, Italy, through the FIRB project 'Sistemi Miniaturizzati per Elettronica e Fotonica'. We are grateful Mr. Roberto Calzolai (Optical Shop, IFAC-CNR) for technological assistance.

References

[1] J.S. Wang, E.M. Vogel, E. Snitzer, J.L. Jackel, V.L. da Silva, Y. Silberberg, J. Non-Cryst. Solids 178 (1994) 109.
[2] S.Q. Man, E.Y.B. Pun, P.S. Chung, Opt. Comm. 168 (1999) 369.
[3] M. Naftaly, S. Shen, A. Jha, Appl. Opt. 39 (27) (2000) 4979.
[4] J.S. Wang, E.M. Vogel, E. Snitzer, Opt. Mater. 3 (3) (1994) 187.
[5] A. Mori, T. Sakamoto, K. Kobayashi, K. Shikano, K. Oikawa, K. Hoshino, T. Kanamori, Y. Ohishi, M. Shimizu, J. Lightwave Technol. 20 (5) (2002) 794.
[6] R. Rolli, K. Gatterer, M. Wachtler, M. Bettinelli, A. Speghini, D. Ajò, Spectrochim. Acta Part A 57 (2001) 2009.
[7] L. Le Neindre, S. Jiang, B.C. Hwang, T. Luo, J. Watson, N. Peyghambarian, J. Non-Cryst. Solids 255 (1999) 97.
[8] R. Stegeman, L. Jankovic, H. Kim, C. Rivero, G. Stegeman, K. Richardson, P. Delfyett, Y. Guo, A. Schulte, T. Cardinal, Opt. Lett. 28 (13) (2003) 1126.
[9] S.I. Najafi, Introduction to Glass Integrated Optics, Artech House, 1992.
[10] G.C. Righini, S. Pelli, SPIE Proc. 4453 (2001) 93.
[11] P. Madasamy, G. Nunzi Conti, P. Poyhonen, Y. Hu, M.M. Morrel, D.F. Geraghty, S. Honkanen, N. Peyghambarian, Opt. Eng. 41 (5) (2002) 1084.
[12] Y. Ding, S. Jiang, T. Luo, Y. Hu, N. Peyghambarian, SPIE Proc. 4282 (2001) 23.
[13] E. Chierici. M.C. Didavide, A. Moro, O. Rossotto, L. Tallone, E. Monchiero, IEEE/LEOS Proceedings of Workshop on Fibre and Passive Components, 2002, p. 24.
[14] C.E. Chryssou, F. Di Pasquale, C.W. Pitt, J. Select. Topics Quantum Electron 6 (1) (2000) 114.
[15] G.L. Yip, J. Albert, Opt. Lett. 10 (3) (1985) 151.
[16] B.R. Judd, Phys. Rev. 127 (1962) 750.
[17] G. Nunzi Conti, V.K. Tikhomirov, M. Bettinelli, S. Berneschi, M. Brenci, B. Chen, S. Pelli, A. Speghini, A.B. Seddon, G.C. Righini, Opt. Eng. 42 (10) (2003) 2805.
[18] V.K. Tikhomirov, A.B. Seddon, D. Furniss, M. Ferrari, J. Non-Cryst. Solids 326–327 (2003) 296.